

HMT-Grasp: A Hybrid Mamba-Transformer Approach for Robot Grasping in Cluttered Environments

Songsong Xiong¹, Hamidreza Kasaei¹

Abstract—Robot grasping, whether handling isolated objects, cluttered items, or stacked objects, plays a critical role in industrial and service applications. However, current visual grasp detection methods based on Convolutional Neural Networks (CNNs) and Vision Transformers (ViTs) often struggle to adapt to diverse scenarios, as they tend to emphasize either local or global features exclusively, neglecting complementary cues. In this paper, we propose a novel hybrid Mamba-Transformer approach to address these challenges. Our method improves robotic visual grasping by effectively capturing both global and local information through the integration of Vision Mamba and parallel convolutional-transformer blocks. This hybrid architecture significantly improves adaptability, precision, and flexibility across various robotic tasks. To ensure a fair evaluation, we conducted extensive experiments on the Cornell, Jacquard, and OCID-Grasp datasets, ranging from simple to complex scenarios. Additionally, we performed both simulated and real-world robotic experiments. The results demonstrate that our method not only surpasses state-of-the-art techniques on standard grasping datasets but also delivers strong performance in both simulation and real-world robot applications.

I. INTRODUCTION

Robotic grasping is a fundamental capability for autonomous manipulation in industrial automation, service robotics, and domestic applications [1], [2]. Robots operate in real-world situations where objects vary in shape, size, and material properties and are randomly arranged and partially occluded. In such challenging conditions, robust and adaptive grasping strategies are needed to identify feasible grasp configurations despite significant visual and physical clutter [3].

Conventional approaches to robotic grasping relied on analytical methods and hand-crafted features, which performed adequately under controlled conditions but failed to generalize to complex, unstructured environments. With the advent of deep learning, convolutional neural networks (CNNs) have become the predominant paradigm for extracting discriminative local features that are essential for grasp detection [4]–[8]. However, in cluttered scenes, local features alone are often insufficient because grasping decisions depend critically on global contextual cues—such as spatial relationships among objects and prevalent occlusion patterns—which traditional CNNs may not adequately capture. Recently, transformer architectures have underscored their ability to model long-range dependencies and provide a more

comprehensive contextual representation [9], [10]. Nonetheless, these methods may inadvertently diminish the local spatial details—such as edges, corners, and shapes—that are crucial for accurate grasp detection [11]. In contrast, recent advances in Mamba architectures extract both local and global features in a more balanced manner than ViTs and CNNs [12], [13], which tend to favor one over the other, thereby mitigating their limitations.

To improve robot grasp detection performance in multiple scenarios, we propose a novel Mamba-Transformer architecture that leverages a state space model (SSM) to fuse and refine features extracted by parallel CNN and Transformer modules. By effectively integrating local detail with global contextual cues, our approach facilitates robust grasping detection across various scenes. Experimental results show that our method outperforms state-of-the-art techniques on multiple grasping datasets and delivers superior performance in both simulation and real-world robotic applications. The main contributions of this paper are summarized as follows:

- 1) We propose a hybrid Mamba-Transformer architecture that integrates parallel CNN and Transformer streams, leveraging their respective strengths to enable the simultaneous extraction of fine-grained local features and global contextual cues for grasp detection.
- 2) We then present the Mamba encoder to further fuse local and global features, which refines fine local details while effectively integrating broader contextual information.
- 3) We conduct comprehensive evaluations and rigorous ablation studies across multiple grasping datasets, achieving excellent performance. Additionally, we carry out extensive simulation and real robot experiments. The experimental results clearly demonstrate that our approach exhibits robust performance.

II. RELATED WORK

This section mainly reviews recent advancements in robotic grasp detection. Current research on robot grasp detection is primarily categorized into two approaches: CNN-based methods and ViT-based methods. Additionally, we provide a brief overview of recent progress with Vision Mamba in various domains.

A. Grasp Detection

CNN-Based Methods: Convolutional Neural Networks (CNNs) have been widely applied in robotic visual grasping tasks [7]. Early work by Lenz et al. introduced a two-step cascaded system that employed two deep neural networks to

¹Department of Artificial Intelligence, University of Groningen, Groningen, The Netherlands
{s.xiong, hamidreza.kasaei}@rug.nl

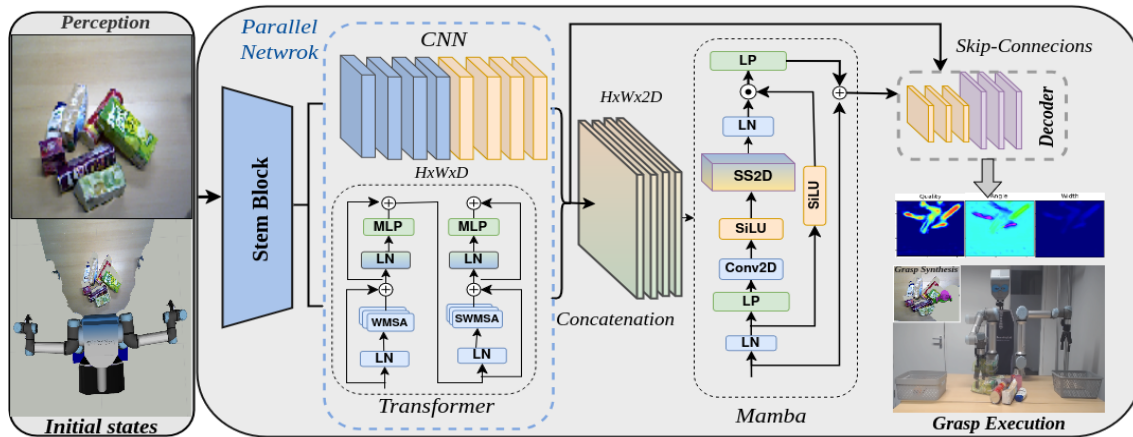


Fig. 1: Overview of the hybrid mamba-transformer architecture for robotic grasping in cluttered environments: The system comprises a grasp encoder, which integrates parallel CNN and transformer networks, followed by mamba blocks for enhanced feature fusion. A grasp decoder with skip connections further refines local and global feature extraction. The decoder upsamples to predict grasp quality, angle, and width, forming the grasp synthesis. Finally, based on the synthesized grasp prediction, the robot executes the grasp.

predict the grasp pose of objects. In this approach, numerous candidate grasps are first generated and then re-evaluated in a second step, which significantly slows down the detection process [9]. Subsequent research has leveraged CNNs to enhance object grasping performance by predicting grasp rectangles. Redmon et al. proposed a single-stage regression model that enabled real-time grasp detection [6]. To further improve accuracy, a ResNet-50-based grasp detector was introduced, demonstrating superior performance on the Cornell RGB-D dataset [14]. Datasets such as Jacquard [15] and Multi-Object [16] have contributed to enhancing the accuracy and generalization of CNN models in grasp detection. In addition, the Generative Grasping CNN (GG-CNN), designed to work with depth images, improved pixel-wise grasp quality in real-time scenarios. GR-ConvNet [8], proposed by Kumra et al., used n -channel inputs to detect antipodal grasps, achieving high accuracy on the Cornell and Jacquard datasets. Despite the effectiveness of CNN-based methods in grasp detection, a significant drawback is their tendency to lose global context due to the inherent structure of stacked convolutional layers [9].

ViT-Based Methods: Motivated by the success of Vision Transformers (ViTs) in object detection and image classification, researchers are increasingly exploring their potential for predicting object grasp poses in robotic tasks [9], [10], [17], [18]. Wang et al. [9] were among the first to propose the use of Swin-Transformers for visual grasp detection, employing them as both encoders and decoders with skip connections to generate pixel-level grasp representations. Building on this, Dong et al. [10] also utilized Swin-Transformers for encoding, coupled with fully convolutional decoders to enhance grasp detection performance. In a more recent effort, Yenicesu et al. [18] introduced LITV2, a lightweight ViT model, to achieve real-time grasp detection. Compared to CNN-based methods, ViT-based approaches have demon-

strated improved grasp detection accuracy. However, as the depth of transformer blocks increases, local-level information tends to gradually diminish [11].

B. Visual Mamba

Recently, Mamba, a novel State Space Model (SSM) initially developed for natural language processing (NLP) [19], has shown strong potential for efficiently modeling long sequences. This success has sparked increasing interest in applying SSMs to visual tasks. In particular, Mamba has been successfully implemented in various computer vision applications. For example, ViM [20], a Mamba-based architecture, operates on image patch sequences using a 1D causal scanning mechanism. However, the 1D scanning approach faces challenges in fully capturing global representations. To address this limitation, VMamba [21] introduces 2D-Selective-Scan, transforming images into sequences of patches for improved global feature extraction.

Inspired by these advancements, SegMamba [22] and VM-UNet [23] have successfully integrated visual state space models into encoders for medical image segmentation, contributing to notable performance improvements in this domain. Despite these developments, no prior work has explored the application of SSMs in robotic grasp detection. Given the strengths of mamba in capturing both global information and local details, alongside the complementary capabilities of transformers and CNNs, we designed a Mamba-Transformer approach to predict robotic grasp poses. Our method demonstrates superior grasp success rates compared to state-of-the-art transformer- and CNN-based approaches.

III. METHOD

In this section, we present a hybrid Mamba-Transformer architecture for robotic grasp detection. The overall structure of the proposed model is illustrated in Fig. 1.

A. Grasp Encoder

We first apply a Stem Block comprising two convolutional layers to downsample the input tensor. The resulting feature map is then fed into a parallel network architecture that integrates CNNs and Transformers, as shown in Fig. 1.

1) *Parallel Network*: To capture spatial relationships among objects, we employ the Swin Transformer block [24], which leverages window-based multi-head self-attention (WMSA) and shifted window-based multi-head self-attention (SWMSA). Although window-based attention extracted localized features, shifting windows promote cross-window interactions, thereby enhancing global modeling capability [11]. However, Transformers alone tend to suppress fine-grained local features at increasing depths [11]. To address this limitation, we incorporate convolutional neural networks (CNNs) within the Parallel Network. More specifically, we adopt a dual convolutional architecture [25] to capture localized details such as edges and shapes. This complementary design capitalizes on CNNs’ inherent translation invariance and inductive biases, leading to more robust representations for robotic grasp detection.

2) *Mamba Blocks*: The Mamba Block employs a recursive state space model (SSM) that supports continuous information flow across the spatial domain. Two core mechanisms drive this design: *implicit attention*, which propagates long-range dependencies, and *dynamic filtering*, which adaptively fuses local and global features. When input features combine CNN-derived local details and transformer-based global context, Mamba’s dynamic filtering effectively balances these distinct feature types. Consequently, Vision Mamba achieves an optimal trade-off between preserving local detail and modeling broader structures. This capability enhances the overall feature representation capacity within the Parallel Network.

Following the parallel feature extraction, we concatenate the outputs into x_m^{l-1} of dimension $(B, 2D, W, H)$. Inspired by the VM-UNet architecture [23], we feed this concatenated feature map into the *mamba block*, which comprises *Layer-Norm (LN)*, *Linear Projection (LP)*, *Conv2d*, *SiLU*, and the 2D-Selective-Scan (*SS2D*) mechanism:

$$\begin{aligned} x_m^{l,0} &= \text{LN}(x_m^{l-1}), \\ x_m^{l,1} &= \text{LN}\left(\text{SS2D}\left(\text{SiLU}\left(\text{Conv2d}\left(\text{LP}\left(x_m^{l,0}\right)\right)\right)\right)\right), \\ x_m^l &= \text{LP}\left(\text{SiLU}\left(x_m^{l,0}\right) \odot x_m^{l,1}\right) + x_m^{l-1}. \end{aligned} \quad (1)$$

where \odot indicates element-wise multiplication. The residual connection ensures stable gradient flow, while SS2D promotes richer spatial feature extraction.

B. Grasp Decoder

In the decoder phase, skip connections establish feature reuse by combining encoder outputs with corresponding decoder stages, as shown in Fig. 1. We apply average pooling to the encoder feature maps, then upsample them by a factor of two. A subsequent *DoubleConv* operation reduces channel dimensionality:

$$x_{de}^{up+1} = \text{DoubleConv}\left(\text{UpSample}\left(x_{de}^{up}\right)\right). \quad (2)$$

Through iterative refinement, the decoder progressively restores spatial resolution. Once feature maps reach $(B, 48, 112, 112)$, they are upsampled again to yield pixel-level heatmaps matching the original image resolution of 224×224 . These heatmaps include a grasp confidence map Q , a gripper angle map Θ , and a gripper width map W .

C. Grasp Synthesis

A robotic antipodal grasp can be defined by the tuple, $g_i = (\langle u, v \rangle, \phi, w, q_i)$ where $\langle u, v \rangle$ denotes the grasp center in pixel coordinates, $\phi \in [-\frac{\pi}{2}, \frac{\pi}{2}]$ is the in-plane rotation, w is the gripper width, and $q_i \in [0, 1]$ indicates the predicted grasp success confidence. Once the pixel $\langle u, v \rangle$ maximizing q_i is found, its location is converted to Cartesian coordinates via known camera intrinsics and a calibrated transformation from the camera to the robot reference frame.

Next, the depth information at $\langle u, v \rangle$ is extracted to determine the object’s position along the optical axis. To ensure robust execution of the grasp, the system may also consider a small neighborhood around the selected pixel to accommodate variations in sensor noise or object geometry. Finally, the manipulator is instructed to close the gripper at the computed position and orientation, thereby completing the grasp action.

IV. EXPERIMENTS

In this section, we present a comprehensive evaluation of our method through experiments on the Cornell [14], Jacquard [15], and OCID-Grasp [26] datasets. We evaluate the impact of skip connections, perform an ablation study on multiple components, and compare our approach against state-of-the-art methods. Additionally, we validate our method in both simulation and real-world robotic experiments. The grasp network has been implemented using PyTorch 2.0.1 with cuDNN 8.5.0.96 and CUDA 11.8. The model is trained end-to-end on an Nvidia RTX 4060 Ti GPU with 16GB of memory.

A. Dataset and Experiment setup

This section outlines the datasets used in the evaluation and provides relevant training details.

1) *Cornell Dataset and Training*: The Cornell dataset is one of the most widely used benchmarks for robotic grasping. It consists of 885 images of 250 real, graspable objects with a total of 8019 annotated grasps. The dataset contains RGB-D images and can be split using two different methods: image-wise and object-wise. Given the relatively small size of the Cornell dataset, we employ 5-fold cross-validation to train and evaluate our model. To ensure robust performance, data augmentation is applied during training. The model is optimized using the Adam optimizer, with a learning rate initialized at 0.0002 and a batch size of 8. Training is carried out over 100 epochs to obtain the final model weights.

2) *Jacquard Dataset and Training*: The Jacquard grasp dataset is a large-scale dataset designed for robotic grasping tasks, comprising over 54,000 synthetic RGB-D images of more than 11,000 distinct objects. It includes approximately 1.1 million labeled grasps, generated using a physics-based simulation environment, providing diverse and comprehensive data for training grasping models. We employ image-wise splitting to train and test our network, where 90% of the data is used for training, and the remaining 10% is reserved for testing. While we utilize the Adam optimizer, similar to the Cornell dataset training, we adjust the learning rate to 0.001 and set the batch size to 8. The network is trained over 200 epochs to obtain the final model weights.

3) *OCID Dataset and Training*: The OCID-Grasp dataset is a large-scale, real-world dataset created for robotic grasping in cluttered environments. It contains 1763 selected images with over 75,000 hand-annotated grasp candidates, classified into 31 object categories. The dataset is designed to capture challenging grasping scenarios involving a variety of objects in cluttered settings. We utilize 5-fold cross-validation, as in the Cornell dataset training, to train the networks and report average performance across the folds. The Adam optimizer is employed with a learning rate of 0.001 and a batch size of 8. The network is trained for 80 epochs to achieve the final model weights.

B. Evaluation Metrics

Similar to previous studies [7]–[9], this work evaluates grasp detection using the following criteria:

- **Angle Difference**: The orientation difference between the predicted grasp and the ground-truth is less than 30° .
- **Jaccard Index**: The Jaccard index between the predicted grasp and the ground-truth is greater than 25%.

C. Performance Comparison with State-of-the-Art Methods

1) *Grasping Performance on the Cornell Dataset*: To demonstrate the effectiveness of our approach, we compared it against state-of-the-art methods under consistent training and testing settings across the Cornell, Jacquard, and OCID-Grasp datasets.

We first evaluated our method on the Cornell dataset using 5-fold cross-validation. Table I presents the results for both image-wise (IW) and object-wise (OW) splits. Our proposed approach achieved a detection accuracy of 99.55%, outperforming other state-of-the-art methods in both splits. The superior performance of HMT-Grasp can be attributed to its ability to effectively capture both local and global features, enabling more precise grasp detection even in challenging scenarios. This result illustrates the robustness and effectiveness of our approach across various input data configurations in the Cornell dataset. Additionally, the experimental result also demonstrates that our method achieves good real-time performance on the tested experimental equipment.

2) *Grasping Performance on the Jacquard Dataset*: Data splitting for the Jacquard dataset varies across methods. For example, GGCNN2 uses 95% of the dataset for training,

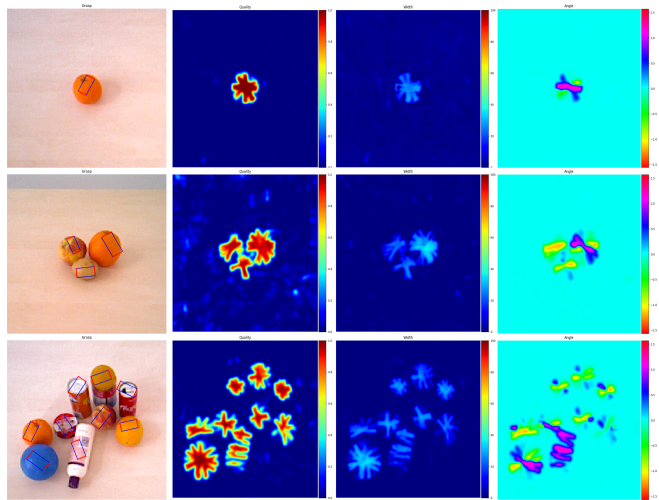


Fig. 2: Multiple-object grasp detection using the HMT. From left to right: grasp rectangles on RGB images, and heatmaps for grasp quality, width, and angle.

while TF-Grasp and GR-ConvNet use 90%, with minor differences in test splits. Additionally, distinctions between image-wise and object-wise splits are often unclear. To ensure fair comparisons, we reran all Jacquard experiments following the same protocol as state-of-the-art methods. The training and evaluation protocol is detailed in the *Jacquard Dataset and Training* section. As shown in Table II, our HMT-Grasp approach, using RGB-D input, achieved 93.3% accuracy, surpassing existing methods. The consistent improvement across different data splits reinforces the effectiveness of our hybrid architecture in capturing the critical features required for successful grasp prediction.

3) *Grasping Performance on the OCID-Grasp Dataset*: To validate our method in complex environments, we evaluated it on the OCID-Grasp dataset. The results, presented in Table III, follow the settings outlined in the *OCID*

TABLE I: Results of our methods on the Cornell Grasping Dataset in image-wise and object-wise settings.

Method	Input	Accuracy (%)		Time (ms)
		IW	OW	
GG-CNN [7]	D	73.0	69.0	19
GPRN [27]	RGB	88.7	-	200
HybridGrasp [28]	RGB-D	93.2	89.1	-
GR-ConvNet [8]	RGB	96.6	95.5	19
GR-ConvNet [8]	RGB-D	97.7	96.6	20
TF-Grasp [9]	D	95.2	94.9	41.1
TF-Grasp [9]	RGB	96.78	95.0	41.3
TF-Grasp [9]	RGB-D	97.99	96.7	41.6
HRG-Net [29]	D	99.43	96.8	52.6
HRG-Net [29]	RGB	98.50	96.7	53.0
HRG-Net [29]	RGB-D	99.50	97.5	53.7
AE-GDN [30]	RGB	97.2	96.4	24.6
AE-GDN [30]	RGB-D	98.9	97.9	26.4
DCSFC-Grasp [31]	RGB-D	99.3	98.5	22
CGD-CNN [32]	RGB-D	97.8	96.6	19
QQGNN [1]	RGB-D	97.7	98.9	14.7
HMT-Grasp (Ours)	RGB	99.21	99.44	23.8
	D	99.32	99.55	22.3
	RGB-D	99.55	99.55	24.8

TABLE II: The Accuracy on Jacquard Grasping Dataset.

Reference	Method	Input	Accuracy (%)
Morrison [7]	GGCNN2	RGBD	88.3
Kumra [8]	GR-ConvNet	RGB-D	91.0
Wang [9]	TF-Grasp	RGB-D	86.7
Ours	HMT-Grasp	D	93.0
	HMT-Grasp	RGB	90.4
	HMT-Grasp	RGB-D	93.3

Dataset and Training section. Our approach, using RGB input, outperformed other methods, demonstrating its superior ability to handle complex grasping scenarios, and showing greater adaptability compared to ViTs and CNNs. As shown in Fig 2, the grasping detection results demonstrates our proposed grasp detection method can achieve a good performance across multiple objects scenarios. The superior performance in this cluttered environment underscores the enhanced feature extraction capability of the Mamba blocks, which balance local and global information to enable more effective grasping decisions in difficult scenarios.

D. Ablation Studies

To further investigate the impact of skip-connections and the Mamba block on grasp pose learning, we trained our network using 5-fold cross-validation on the Cornell dataset with image-wise splitting.

1) *Ablation study for skip-connections:* We firstly conducted experiments with and without skip-connections using our method across RGB, Depth, and RGB-D inputs. The detailed experimental results are presented in Table IV. The study results indicate that incorporating skip connections improves grasp detection performance, particularly for RGB-based inputs, achieving a 2.3% improvement compared to the absence of skip connections.

2) *Ablation study for different components:* To evaluate the contributions of the CNN, Transformer, and Mamba modules in our proposed method, we conduct an ablation study on the OCID-Grasp dataset. The results are presented in Table V. As shown in the first row, using CNN-only achieves accuracy of 73.9%. When replacing the CNN with only the Transformer and Mamba modules, the accuracy drops to 71.2%, indicating that the convolutional network captures essential local grasping features, such as the textures and edge, as shown in Fig. 3 that significantly contribute to detection performance.

TABLE III: The Accuracy on OCID-Grasp Grasping Dataset.

Reference	Method	Input	Accuracy (%)
Morrison [7]	GGCNN2	D	69.3
	GGCNN2	RGB	65.7
	GGCNN2	RGBD	67.6
Kumra [8]	GR-ConvNet	D	70.0
	GR-ConvNet	RGB	68.5
	GR-ConvNet	RGB-D	72.3
Wang [9]	TF-Grasp	D	72.0
	TF-Grasp	RGB	58.9
	TF-Grasp	RGB-D	61.8
Ours	HMT-Grasp	D	73.5
	HMT-Grasp	RGB	76.5
	HMT-Grasp	RGB-D	74.1

TABLE IV: Ablation experimental results from different skip-connections on the OCID-Grasp dataset.

Modality	Connections	With	Without
	Skip-connections	Skip-connections	Skip-connections
Depth(%)		73.5	73.1
RGB(%)		76.5	74.2
RGB-D(%)		74.1	73.4

When combining the CNN with the Mamba module, the accuracy remains at 73.9%, showing no substantial improvement compared to using only the CNN or Mamba. As shown in Fig. 3, the quality heatmaps of Mamba-only and CNN-only models indicate that both focus more on local details compared to the Transformer-only model. This also suggests that while Mamba effectively enhances sequence modeling, it lacks the capability to fully compensate for the absence of strong global representations, which are crucial in complex, multi-object grasping scenarios where spatial relationships between objects and background diversity play a significant role. In contrast, the combination of the CNN and Transformer results in a slight performance drop compared to the standalone components. This outcome underscores the importance of the Mamba module in balancing local and global representations. The Mamba module refines feature extraction by integrating local information from the CNN and global spatial awareness from the Transformer, ensuring that the model does not overly prioritize one type of representation at the expense of the other.

Finally, our method, which integrates CNN, Transformer, and Mamba, achieves the highest accuracy of 76.5%, demonstrating Mamba’s effectiveness in furthering refine local and global features for enhanced grasp detection. These results validate our architecture. CNN primarily captures fine local details, the Transformer focuses on extracting global context, and Mamba effectively fuses and enhances both, ultimately improving overall performance.

TABLE V: Ablation study on the OCID-Grasp dataset illustrating the contribution of the CNN, Transformer, and Mamba modules.

Ablation Settings			Accuracy(%)
CNN	Transformer	Mamba	
✓			73.9
	✓		74.0
		✓	74.1
✓	✓		72.7
	✓	✓	71.2
✓		✓	73.9
✓	✓	✓	76.5 (Ours)

E. Simulation and Real Robot Experiments

In this section, we first conducted robot grasping experiments in the Gazebo using models, as shown in Fig. 5. First, we performed 20 isolated experiments for each object by randomly spawning it within the robot’s workspace. The results, presented in Table VI, demonstrate the effectiveness of our method in grasping various objects. The results

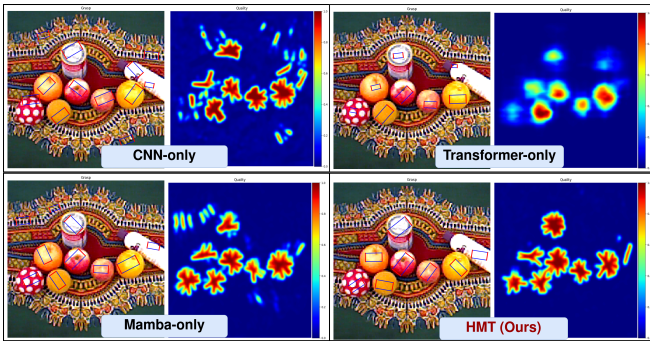


Fig. 3: Comparison of grasp detection outcomes and quality across CNN, Transformer, Mamba, and HMT methods in complex multi-object scenes.

show that HMT-Grasp generally outperforms other methods across most objects. It achieved 100% success on the pear, surpassing GR-ConvNet (80%) and TF-Grasp (85%). It also performed well on can_coke (95%), exceeding all other methods. Although HMT-Grasp generally performed better, there were cases where the improvement was marginal. For example, HMT-Grasp and GR-ConvNet both reached 85% on the banana, and the performance difference for the peach was only 5%. The reasons for failures can be attributed to the complexity of object shapes, material and collision mesh properties. For example, objects like the mug had lower success rates for both methods. The challenge with grasping this object lies in the difficulty of detecting stable grasp points, as small surface areas reduce friction and stability.

We conducted real-robot experiments in lightly, moderately, and heavily cluttered environments with complex backgrounds, as illustrated in Fig. 4. In the lightly cluttered setting, we tested twenty groups of five randomized objects per method to ensure diverse grasping scenarios. In the moderately cluttered setting, we conducted ten groups of ten randomized objects per method to evaluate grasping performance across various backgrounds. In the highly cluttered setting, we ran five experimental groups, each aiming to include twenty distinct objects to assess robustness under dense clutter. We compute the success rate as the ratio of

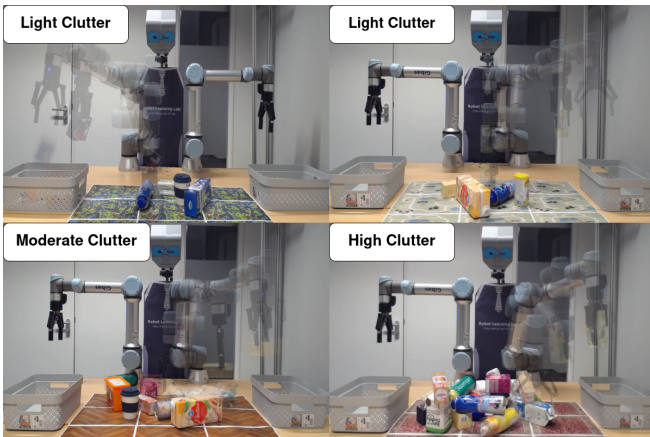


Fig. 4: Experimental setups for robotic grasping with varying clutter: Light, Moderate, and High.

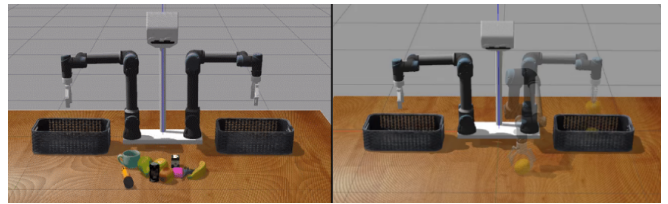


Fig. 5: Simulation setups: (left) all simulation objects; (right) our robot grasps and releases a randomly placed object.

successful grasps to the total number of grasp attempts. The results are presented in Table VII. Overall, our approach consistently showed better performance compared to the baseline methods. However, accuracy decreased from lightly to heavily cluttered scenarios for two primary reasons: (1) insufficient friction between the gripper jaws and certain smooth-surfaced objects, resulting in grasp failures; and (2) the inaccurate grasp prediction led to contacting the gripper with the neighboring objects, resulting in a grasp failure.

TABLE VI: Simulation results: 20 simulations were performed for each object to assess the grasp success rate (%)

Objects	Pear	lemon	sponge	can_coke	Peach
GR-ConvNet [8]	80	75	85	80	75
TF-Grasp [9]	85	70	70	85	70
HMT-Grasp	100	95	75	95	80
Objects	mug	scissor	tea_box	banana	flash
GR-ConvNet [8]	80	70	70	85	75
TF-Grasp [9]	75	85	80	75	80
HMT-Grasp	70	95	80	85	90

TABLE VII: Real-world robot grasp success rates in lightly, moderately, and highly cluttered scenarios.

Models	Success Rate (%)		
	Light Clutter (5 Objects)	Moderate Clutter (10 Objects)	High Clutter (20 Objects)
GR-ConvNet [8]	80	74	72
TF-Grasp [9]	82	75	70
HMT-Grasp	88	82	79

V. CONCLUSION

This paper presents a hybrid Mamba-Transformer model for robotic grasping in complex scenarios. By combining Mamba, Transformers, and CNNs, our method improves the performance of ViTs and CNNs in visual grasp detection. We conducted extensive evaluations on the Cornell, Jacquard, and OCID-Grasp datasets, where our model consistently outperformed state-of-the-art methods, achieving an accuracy of 99.5% on the Cornell dataset. These results demonstrate the superior adaptability and precision of our approach. Additionally, real-world robotic experiments further validated the method’s effectiveness in complex environments, highlighting its potential for practical applications. Future work could focus on incorporating real-time feedback mechanisms to adjust grasp plans dynamically during execution.

REFERENCES

- [1] K. Fu and X. Dang, "Light-weight convolutional neural networks for generative robotic grasping," *IEEE Transactions on Industrial Informatics*, 2024.
- [2] D. Liu, X. Tao, L. Yuan, Y. Du, and M. Cong, "Robotic objects detection and grasping in clutter based on cascaded deep convolutional neural network," *IEEE Transactions on Instrumentation and Measurement*, vol. 71, pp. 1–10, 2021.
- [3] J. Zhao, L. Ye, Y. Wang, and H. Min, "Robot grasping using dilated residual convolutional neural network," in *2022 WRC Symposium on Advanced Robotics and Automation (WRC SARA)*. IEEE, 2022, pp. 133–139.
- [4] Y. Jiang, S. Moseson, and A. Saxena, "Efficient grasping from rgbd images: Learning using a new rectangle representation," in *2011 IEEE International conference on robotics and automation*. IEEE, 2011, pp. 3304–3311.
- [5] I. Lenz, H. Lee, and A. Saxena, "Deep learning for detecting robotic grasps," *The International Journal of Robotics Research*, vol. 34, no. 4-5, pp. 705–724, 2015.
- [6] J. Redmon and A. Angelova, "Real-time grasp detection using convolutional neural networks," in *2015 IEEE international conference on robotics and automation (ICRA)*. IEEE, 2015, pp. 1316–1322.
- [7] D. Morrison, P. Corke, and J. Leitner, "Learning robust, real-time, reactive robotic grasping," *The International journal of robotics research*, vol. 39, no. 2-3, pp. 183–201, 2020.
- [8] S. Kumra, S. Joshi, and F. Sahin, "Antipodal robotic grasping using generative residual convolutional neural network," in *2020 IEEE/RSJ International Conference on Intelligent Robots and Systems (IROS)*. IEEE, 2020, pp. 9626–9633.
- [9] S. Wang, Z. Zhou, and Z. Kan, "When transformer meets robotic grasping: Exploits context for efficient grasp detection," *IEEE robotics and automation letters*, vol. 7, no. 3, pp. 8170–8177, 2022.
- [10] M. Dong, Y. Bai, S. Wei, and X. Yu, "Robotic grasp detection based on transformer," in *International Conference on Intelligent Robotics and Applications*. Springer, 2022, pp. 437–448.
- [11] M. Raghu, T. Unterthiner, S. Kornblith, C. Zhang, and A. Dosovitskiy, "Do vision transformers see like convolutional neural networks?" *Advances in Neural Information Processing Systems*, vol. 34, pp. 12 116–12 128, 2021.
- [12] R. Xu, S. Yang, Y. Wang, B. Du, and H. Chen, "A survey on vision mamba: Models, applications and challenges," *arXiv preprint arXiv:2404.18861*, 2024.
- [13] J. Ruan and S. Xiang, "Vm-unet: Vision mamba unet for medical image segmentation. arxiv 2024," *arXiv preprint arXiv:2402.02491*.
- [14] S. Kumra and C. Kanan, "Robotic grasp detection using deep convolutional neural networks," in *2017 IEEE/RSJ International Conference on Intelligent Robots and Systems (IROS)*. IEEE, 2017, pp. 769–776.
- [15] A. Depierre, E. Dellandréa, and L. Chen, "Jacquard: A large scale dataset for robotic grasp detection," in *2018 IEEE/RSJ International Conference on Intelligent Robots and Systems (IROS)*. IEEE, 2018, pp. 3511–3516.
- [16] F.-J. Chu, R. Xu, and P. A. Vela, "Real-world multiobject, multigrasp detection," *IEEE Robotics and Automation Letters*, vol. 3, no. 4, pp. 3355–3362, 2018.
- [17] Y. Han, R. Batra, N. Boyd, T. Zhao, Y. She, S. Hutchinson, and Y. Zhao, "Learning generalizable vision-tactile robotic grasping strategy for deformable objects via transformer," *arXiv preprint arXiv:2112.06374*, 2021.
- [18] A. S. Yenesu, B. Cicek, and O. S. Oguz, "Fvit-grasp: Grasping objects with using fast vision transformers," *arXiv preprint arXiv:2311.13986*, 2023.
- [19] A. Gu and T. Dao, "Mamba: Linear-time sequence modeling with selective state spaces. arxiv 2023," *arXiv preprint arXiv:2312.00752*.
- [20] L. Zhu, B. Liao, Q. Zhang, X. Wang, W. Liu, and X. Wang, "Vision mamba: Efficient visual representation learning with bidirectional state space model," 2024. [Online]. Available: <https://arxiv.org/abs/2401.09417>
- [21] Y. Liu, Y. Tian, Y. Zhao, H. Yu, L. Xie, Y. Wang, Q. Ye, and Y. Liu, "Vmamba: Visual state space model," 2024. [Online]. Available: <https://arxiv.org/abs/2401.10166>
- [22] Z. Xing, T. Ye, Y. Yang, G. Liu, and L. Zhu, "Segmamba: Long-range sequential modeling mamba for 3d medical image segmentation," 2024. [Online]. Available: <https://arxiv.org/abs/2401.13560>
- [23] J. Ruan and S. Xiang, "Vm-unet: Vision mamba unet for medical image segmentation," 2024. [Online]. Available: <https://arxiv.org/abs/2402.02491>
- [24] Z. Liu, Y. Lin, Y. Cao, H. Hu, Y. Wei, Z. Zhang, S. Lin, and B. Guo, "Swin transformer: Hierarchical vision transformer using shifted windows," in *Proceedings of the IEEE/CVF international conference on computer vision*, 2021, pp. 10 012–10 022.
- [25] O. Ronneberger, P. Fischer, and T. Brox, "U-net: Convolutional networks for biomedical image segmentation," in *Medical image computing and computer-assisted intervention–MICCAI 2015: 18th international conference, Munich, Germany, October 5-9, 2015, proceedings, part III 18*. Springer, 2015, pp. 234–241.
- [26] S. Ainetter and F. Fraundorfer, "End-to-end trainable deep neural network for robotic grasp detection and semantic segmentation from rgb," in *2021 IEEE International Conference on Robotics and Automation (ICRA)*. IEEE, 2021, pp. 13 452–13 458.
- [27] H. Karaoguz and P. Jensfelt, "Object detection approach for robot grasp detection," in *2019 International Conference on Robotics and Automation (ICRA)*. IEEE, 2019, pp. 4953–4959.
- [28] D. Guo, F. Sun, H. Liu, T. Kong, B. Fang, and N. Xi, "A hybrid deep architecture for robotic grasp detection," in *2017 IEEE International Conference on Robotics and Automation (ICRA)*. IEEE, 2017, pp. 1609–1614.
- [29] Z. Zhou, S. Wang, Z. Chen, M. Cai, and Z. Kan, "A robotic visual grasping design: Rethinking convolution neural network with high-resolutions," *arXiv preprint arXiv:2209.07459*, 2022.
- [30] X. Qin, W. Hu, C. Xiao, C. He, S. Pei, and X. Zhang, "Attention-based efficient robot grasp detection network," *Frontiers of Information Technology & Electronic Engineering*, vol. 24, no. 10, pp. 1430–1444, 2023.
- [31] M. Zou, X. Li, Q. Yuan, T. Xiong, Y. Zhang, J. Han, and Z. Xiao, "Robotic grasp detection network based on improved deformable convolution and spatial feature center mechanism," *Biomimetics*, vol. 8, no. 5, p. 403, 2023.
- [32] Y. Gu, D. Wei, Y. Du, and J. Cao, "Cooperative grasp detection using convolutional neural network," *Journal of Intelligent & Robotic Systems*, vol. 110, no. 1, pp. 1–14, 2024.